

Use of the solvent chemistry for the control of the critical thickness of PbTiO₃ ultrathin film

R Fernández¹, S Holgado², Z Huang³, M L Calzada¹, J. Ricote*¹

¹Instituto de Ciencia de Materiales de Madrid, CSIC, Cantoblanco, E-28049 Madrid, Spain

²Escuela Politécnica Superior, Universidad Autónoma de Madrid, Cantoblanco, E-28049 Madrid, Spain

³Department of Materials, School of Applied Sciences, Cranfield University, Bedfordshire MK43 0AL, United Kingdom

*corresponding author

E-mail: jricote@icmm.csic.es

keywords: ferroelectrics, solution deposition, ultrathin films

(To be submitted to J. Mater. Res.)

Abstract. The preparation of high quality ferroelectric PbTiO₃-based ultrathin films by Chemical Solution Deposition, using a diol-based sol-gel method, have proved to be successful. However, there is a critical thickness below which the films break up into isolated structures. According to previous studies, above a certain grain size to thickness ratio a microstructural instability occurs and the deposits are no longer continuous. We explore the use of the solvent chemistry to control this phenomenon, as an alternative to the more conventional variation of the crystallization parameters. The use of diols with short C chain lengths, in the synthesis process of the precursor solutions, leads to films with smaller grain sizes, whose critical thickness are lower. A reduction from 40 to 15 nm is achieved by reducing the number of C of the diol used from 5 to 2. It is concluded that a critical value of $G/t < 5.0$ is necessary to obtain continuous ultrathin films with the processing conditions used.

1. Introducción

The present miniaturization trends in the microelectronics industry, is demanding an ever larger degree of integration. Device dimensions are now in the nanometre scale, and, thus, all the elements that are part of them. This size reduction can be a challenge in some cases, like for Nanoelectromechanical Systems (NEMS), as most of the techniques used for transduction reach their limits in the nanoscale [1]. The use of ultrathin ferroelectric films, with large piezoelectric coefficients, is a good option to be explored. Besides, ultrathin films are required for writing thermally stable domains for probe-based data ferroelectric storage devices [2], which to be of a uniform size must be large relative to the grain size [3]. So the challenge is producing ultrathin ferroelectric films with small grain size. However, further development in the fabrication methods of ferroelectric oxide nanostructures to be integrated in the new nanodevices is necessary, not only because of the potential technological interest [4], but also because of the unique properties of ferroelectrics with reduced dimensions [5-8].

Chemical Solution Deposition (CSD) presents clear advantages over other methods of preparation of high quality ferroelectric films for their integration in nanodevices. The high degree of compositional control achieved, the large deposition areas and the low costs have made them the method of preparation of a wide range of oxide films for electronic applications [9]. However, they have been regarded traditionally as unsuitable for the deposition of ultrathin films (below 100 nm thickness), and other deposition techniques as pulsed laser deposition or chemical vapour deposition are often used to prepare them. Regardless of that, ultrathin films have been successfully obtained by CSD methods: both of non-ferroelectric [10,11] and

ferroelectric [12-17] compositions, with thickness as low as 9 nm, as has been reported recently [18].

However, there is a serious problem concerning the loss of continuity in films with reduced thickness. Based on previous observations, Millar and Lange developed a model [19], which predicts that, above a critical value of the grain size to thickness ratio (G/t), a microstructural instability occurs, and films break up into separated structures. Thickness reduction leads normally to a situation in which grains reach similar dimensions to film thickness. Grain growth is then restricted to the plane of the film, which results in grains with lateral dimensions (G) larger than film thickness (t). At some point, grain growth is no longer a mechanism for energy reduction, and a process of spheroidization of the grains starts, which produces a deterioration of the uniformity of the film. This can result, for small thickness, that, between two grains, pinholes to the substrate are formed. And, above a critical value of G/t , grains form isolated structures and the film is no longer continuous. This model has been confirmed experimentally on studies of several very thin oxide films, which become discontinuous when their grains grow as a result of the use of higher crystallization temperatures [20-24]. Similarly, for a series of films with decreasing thickness we can define a critical thickness below which a complete coating of the substrate is not achieved. Figure 1 shows the results of our previous works on the preparation of ultrathin films by chemical solution deposition methods [16,17], and the critical thickness deduced from the analysis carried out on the films. The more diluted is the precursor solution, the thinner is the resulting film. The correlation between these two parameters is broken when a certain critical thickness is reached. The loss of continuity is the reason, and, therefore, the calculated values of thickness from the reflectivity measurements are an average between coated and uncoated areas. It was concluded that there seems to be a critical thickness around 17

nm for all the series of lead titanate based films studied. In this work, we study the role of the solvent chemistry in the preparation of ultrathin films, and its influence on the appearance of the microstructural instability that leads to discontinuous films. Both the solvent used for the dilution of the precursor solution and the type of diol chosen for the synthesis are proved to be relevant to decrease the critical thickness below which the coatings are incomplete.

2. Experimental procedure

Thin films of lead titanate (PbTiO_3) were prepared starting from air-stable precursor solutions obtained by a sol-gel route that uses a diol as solvent [25]. In this work three types of diols (1,3 propanediol, 1,2 etanediol and 1,5 pentanediol) are used alternately to see the influence of the length of the C chain on the properties of the films. The starting reagents used were equimolar concentrations of lead acetate trihydrate, $\text{Pb}(\text{CH}_3\text{COO})_2 \cdot 3\text{H}_2\text{O}$, and titanium diisopropoxide bisacetylacetonate, $\text{Ti}(\text{OC}_3\text{H}_7)_2(\text{CH}_3\text{COCHCOCH}_3)_2$. The diol to Pb/Ti mole ratio used was 5:1. To account for the Pb losses occurring during the crystallization, a 10 mol% excess of PbO was used. The stock solutions were diluted with 2ethyl-1hexanol ($\text{C}_8\text{H}_{18}\text{O}$) to obtain concentrations between 0.30 and 0.0125 M, that allow the preparation of ultrathin films. The diluted solutions were then deposited by spin coating at 2000 rpm for 45 s onto Pt/TiO₂/SiO₂/(100)Si substrates. After the deposition of a single layer, the film is dried at 350°C for 60 s on a hot plate, and then crystallization is carried out by rapid thermal processing at 650°C for 50 s, with a heating rate of $\sim 30^\circ\text{C/s}$.

Aliquots of the precursor solutions with 0.3 M concentrations were dried at 100°C for 12 h in a furnace. The gel powder obtained was studied by Differential Thermal Analysis (DTA) and Thermogravimetric Analysis (TGA) between 25° and 1000°C, at a rate of 10°C/min in a Seiko TG/DTA 320U apparatus.

Grazing incidence X-ray diffraction with a D500 diffractometer (Siemens AG, Berlin-Munich, Germany) at an incident angle of 1° was used to confirm that the films are perovskite single phase. A scanning force microscope (SFM) (Nanotec[®] with WSxM[®] software; Nanotec Electrónica) was used to study the surface topography of the films with the dynamic mode. Film thickness was determined by spectroscopic ellipsometry with a phase-modulated ellipsometer UVISEL (Horiba Iyon SAS) operating between 1.5 and 4.5 eV. To study the films by Transmission Electron Microscopy (TEM), cross sections were prepared using a focused ion beam workstation (FEI FIB2000, Hillsboro, OR) following the so-called lift-out method [26]. A protective layer was deposited onto the surface to avoid damaging the film during the cutting of the thin lamella. Due to the ion beam exposure this layer becomes gradually amorphous in its outer part, although it is still crystalline close to the ultrathin films under study. This can be observed in the TEM images. The cut and freed lamellas were transferred to normal TEM Cu grids with a Narishige micromanipulator (Tokyo, Japan). The samples were studied with a Tecnai-20 FEG TEM (FEI) working at 200 kV.

3. Results and discussion

For the preparation of ultrathin films it is necessary to deposit highly diluted solutions. To study the role of the solvent used for the dilution, we search an alternative

solvent to those traditionally used, diol or water, both already present in the synthesis step. Among organic solvents, ethylhexanol provides, in principle, excellent characteristics for the dilution of the sol-gel derived solutions. Figure 1 shows the evolution of the film thickness with the concentration of the precursor solution for PbTiO₃-based films. Together with results previously reported of films for which precursor solutions are diluted either in diol or water [16,17], we include a new series obtained from solutions diluted in ethylhexanol. We observe the same trend in all of them: a correlation between the thickness and the molar concentration that is lost in the thinnest films. We found that the reason is that below a critical value films become discontinuous. The only difference is that precursor solutions diluted in ethylhexanol produce thinner films for the same concentration, which makes ethylhexanol the best option to prepare the thinnest films possible, and the solvent of choice for the dilution of the solutions in this work.

To understand the difference among solutions diluted in different solvents and their influence on the resulting films, the thermal decomposition of their gels is analyzed by DTA and TGA (Figure 2). The curves corresponding to the gels obtained from solutions diluted in diol and water (Figures 2.a and b) show very similar behaviours. In both cases, the highest mass losses take place for temperature below 500°C, at similar positions to the exothermic peaks around 320° and 460°C. In contrast, the gel from the solution diluted in ethylhexanol (Figure 2.c) presents the largest mass loss (37.8%) below 350°C, which is close to an exothermic peak at 316°C. This is an indication that the decomposition of organics takes place at lower temperatures for the solutions diluted in ethylhexanol. The emission of a large percentage of the organics present in the solution at temperatures similar to those used for the drying step (350°C) results in a crystallization of the resulting film with less organic species trapped in its

volume. As a consequence residual porosity must be reduced, promoting a larger degree of densification and lower values of thickness for the same precursor solution concentration. It must be remarked the large influence of organic species in the behaviour of solutions as highly diluted as the ones used to obtain films with thickness below 100 nm. It can be concluded from these results that the films obtained from a single deposit of solutions diluted in solvents that decompose at lower temperatures, like ethylhexanol, can reach lower thickness than those derived from solutions diluted in more conventional solvents, like water or diol.

However, the critical thickness seems to be unaltered, regardless of the solvent used for dilution (Figure 1). In order to obtain even thinner continuous films, an alternative strategy to reduce the critical thickness must be sought. It has been shown that when the grain size to thickness ratio (G/t) is above a critical value, grains become isolated structures, and films are no longer continuous. Therefore, to obtain complete coatings for lower critical thickness [it](#) is necessary to reduce the grain size. The most obvious option is the reduction of the crystallization temperature. We are already using low processing temperatures for the fabrication of the PbTiO_3 films, and a further reduction leads to the appearance of undesirable non-ferroelectric pyrochlore phases. We propose in this work to make use again of the solvent chemistry, specifically of the influence of the type of diol used as a solvent during the synthesis process.

Previous studies carried out on thin films obtained from solutions synthesised by the diol route suggest that variations of the type of diol used can have significant influence on the thickness [27] and the grain size [28]. It was found that the reduction of the length of the C chain of the diol leads to a decrease of the grain size. This result provides the basis for a potential method of controlling the critical thickness through simple modifications of the solvent chemistry.

To evaluate this effect, ultrathin films were prepared from highly diluted PbTiO_3 solutions, synthesized with different diols: 1,2 etanediol, 1,3 propanediol and 1,5 pentanediol. Dilutions were carried out in ethylhexanol. The resulting films are perovskite single phase according to the grazing incidence X-ray diffraction diagrams shown in Figure 3. Most of the reflections come from the perovskite phase, except the 111 from the Pt bottom electrode. Similarly to our previous reported results on ultrathin films, 001 and 002 reflections are not observed, that may be due to a preferential crystallographic orientation present in the film. However, this requires further systematic texture analysis as GIXRD can be misleading. The evolution of film thickness with the concentration of the precursor solution for each series of films is shown in Figure 4. Contrary to the results reported in [27], no clear correlation between film thickness and the type of diol used for the synthesis of the solution is found. Moreover, for the thinnest films the differences observed are insignificant. This result shows that, in the case of highly diluted solutions, the parameter that determines the thickness of the derived films is mainly the dilution of the precursor solutions, which, besides, in all the films studied here is carried out in the same solvent: ethylhexanol.

In order to study the effect of the use of different types of diol on the grain size of the resulting films, and, ultimately, on their continuity, an analysis of the film surfaces is carried out by Scanning Force Microscopy. The images are collected in Figures 5-7. In all of them, an initial decrease of the grain size as thickness is reduced is observed. And, as expected, for some of the thinnest films an incomplete coating of the substrate start to be evident. As expected, the observed grain sizes of the films obtained from solutions synthesized with etanediol (Figure 5) are generally smaller than those of the other two series of films. Grain size is reduced gradually from $\approx 80\text{-}150$ nm diameter of the thickest film (Figure 5.a) to $\approx 40\text{-}100$ nm of the 15 nm thick film (Figure

5.c). An even larger decrease of the concentration of the precursor solution (0.05M) produces incomplete coatings of the substrate (Figure 5.d). When a diol with more C is used, propanediol, (Figure 6) the films derived start to be discontinuous for depositions of solutions of 0.10 M (Figure 6.c), which is more evident if we reduced further the concentration to 0.05 M (Figure 6.d). The continuous films (Figure 6.a and b) have similar thickness, 24 and 19 nm, respectively, and, therefore, show also grains of similar size (\approx 60-150 nm diameter). The occurrence of incomplete coatings is observed for the films derived from solutions 0.15 M when pentanediol is used during the synthesis (Figure 7). In this case the grain size is the larger of the three series: \approx 125-250 nm for the film 40 nm thick (Figure 7.a). Gradually, as concentration of the precursor solution decreases, the regions of substrate without any coating become larger.

From these results we can conclude that an increase of the length of the C chain of the diol used during the synthesis process of the precursor solution produces films with larger grain size for the same processing conditions, being determinant for the complete coating of the substrate.

Although these studies of the film surfaces by SFM give information about the continuity of the films, in some cases they are not conclusive. It has to be considered that films are deposited on polycrystalline Pt, whose grains can be mistaken for those of the PbTiO_3 film. In order to have a more clear picture of the evolution of the films when thickness is reduced, and determine the critical thickness below which the films break up into isolated structures, transmission electron microscopy studies of cross sections of the films are carried out. The results are shown in Figures 8-10. In all the micrographs the different layers of the substrate ($\text{Pt/TiO}_2/\text{SiO}_2/\text{Si}$) and the protective layer, used for the preparation of the TEM specimens, are marked.

The deposition of a solution 0.20 M obtained using etanediol produces a continuous film with a thickness of 30 nm, according to the micrographs obtained by TEM of their cross sections (Figure 8.a.). Grain boundaries have not a clear contrast, but it can be deduced that the lateral dimensions of the grains are around 100 nm. These results confirm the ones obtained by ellipsometry and scanning force microscopy shown before. A decrease of the concentration of the precursor solution (0.10 M) produces films with a more irregular thickness, as it can be seen in Figure 8.b. Thickness in this case is around 15 nm, similar to the one obtained by ellipsometry, but with variations between 6 and 23 nm in different regions of the film. The thickness variations are even more important for films prepared from more diluted solutions, 0.05 M (Figure 8.c). Although the coating seems to cover most of the substrate, if we look in detail, we will observe that between grains the films is almost lost, which correspond to the regions without coating observed by SFM of the surface (Figure 6.d). It must be remarked the spheroidization of the grains, which was predicted for stages previous to the separation of the film into isolated structures. The height of the grains (inset) of ~11 nm does not correspond to the value obtained by ellipsometry (8 nm). This shows that the thickness values obtained by this techniques for these films correspond to an average between regions with and without film. Therefore, this latter film cannot be considered continuous. From these observations we can conclude that in the case of films derived of the use of etanediol, and at the processing conditions used here, the critical thickness is close to 14 nm, which is obtained in a film obtained from a 0.10 M solution.

When propanediol is used instead during the synthesis step of the precursor solution, the resulting films show homogeneous thickness for the thicker films (Figure 9.a). When the concentration of the precursor solution is lower, 0.10 M, the resulting film (Figure 9.b) shows higher inhomogeneity of the thickness, which leads to a loss of

coating in some regions. More separated structures (marked with arrows) are observed when the concentration of the precursor solution decreases to 0.05 M (Figure 9.c). These results confirm the trend observed in the SFM experiments (Figure 6.c and d). From the analysis of the images, we can conclude that the critical thickness for films obtained from solutions synthesized with propanediol, at the specified processing conditions, is around 19 nm. It must be noted that it is higher than the one found for the previous films, when etanediol is used instead.

Finally, the use of pentanediol during the synthesis of the precursor solution results in a continuous film when a 0.20 M solution is deposited (Figure 10.a.). Small variations in thickness are observed, which results in an irregular surface and is an indication that it is in a stage previous to the breaking up of the film. Grains are easily identified in the micrographs, whose size is larger than in the previous sets of films, with lateral dimensions between 80 and 200 nm, similar to the values observed by SFM (Figure 7.a). The heights of the grains (30-60 nm) are also in agreement with the average thickness obtained by ellipsometry (40 nm). A small reduction of the concentration of the precursor solution to 0.15 M produces discontinuous films (Figure 10.b). The isolated grains have lateral dimensions between 70 and 125 nm. Similar results are obtained for the film obtained from a 0.10 M solution (Figure 10.c). In this latter case the heights of the grains are a lower (20-30 nm vs. 30-40 nm), as expected when the concentration of the precursor solution is reduced. From all the results obtained for these films, we can deduce that, in this case, the critical thickness is much higher than in the previous sets of films: around 40 nm, which proves the large influence of the type of diol used in the synthesis of the precursor solutions on the fabrication of continuous films.

With this study, it has been shown that the use of diols with different C chain length in the synthesis of the precursor solutions has an effect on the grain size of the resulting films, which, in turn, modifies the critical thickness below which it becomes discontinuous. If we compare films derived from solutions with the same concentration, for example, 0.10 M, we can observe that grain size goes from $\approx 50\text{-}110$ nm when etanediol is used (Figure 5.c) to $\approx 80\text{-}150$ nm when pentanediol is used instead (Figure 7.c). The former is a continuous film (Figure 8.b), while the latter is a collection of isolated grains (Figure 10.c). The use of diols with a short C chain favors the continuity of the deposits for the same concentration of the precursor solution. Similarly, the process of spheroidization of the grains in the films takes place for lower concentrations of the precursor solution if a diol with a shorter C chain is used. The critical thickness, that marks the transition from this stage to a discontinuous film goes from 40 nm in the case that the diol used is pentanediol, to 15 nm when etanediol is the choice. In fact, the parameter that controls this variation is the grain size to thickness ratio (G/t). Estimations of G/t values for all the films studied here and in previous works are summarized in Table 1. In all cases thickness obtained by ellipsometry are used, even for discontinuous films. Grain size is estimated from the lateral dimensions of a group of grains obtained from the scanning force microscopy images of the film surfaces. It can be seen that, in general, above $G/t \geq 5.0$ films become discontinuous. Calculations based on energy considerations [19] show that films with $G/t < 8/\pi$ are always continuous. In our case G/t are always above this value, and, therefore, it seems that the degree of spheroidization of the grains rules the process of breaking up of the film. A parameter that is used to describe this [19] is ψ , defined as the angle between the boundaries of two neighboring grains. ψ is equal to π when there is no spheroidization of the grains, and becomes progressively smaller until it reaches a critical value (ψ_{crit}),

below which the neighboring grains separate. ψ_{crit} is directly related to G/t [19]. The value of the angle ψ , is determined by the free energy of the surfaces of film, substrate and grain boundaries, and also the interface substrate-film. Therefore, changes of these surface and interface energies (processing at different atmospheres, deposits on different substrates...) can alter the microstructural stability and the process of separation of the film. In this work, processing parameters have been similar in all cases, except for the choice of solvents, so the variations of the critical values are directly related to the induced variations of the grain size. From our results it seems that for PbTiO_3 films, obtained by Chemical Solution Deposition on platinized Si-based substrates, a critical value of $G/t < 5.0$ is necessary to obtain continuous ultrathin films.

4. Conclusions

This work demonstrates the important role of the solvent chemistry in the preparation of continuous ultrathin films by Chemical Solution Deposition methods. The use of solvents that decompose at lower temperatures, like ethylhexanol, for the dilution of the precursor solutions produces films with lower thickness than the ones obtained with more traditional solvents. This is specially important for ultrathin films, as we use highly diluted solutions to prepare them. We have explored as well the role of the diols used as solvents during the synthesis of the precursor solution, and the results show that they allow a control of the grain size of the films, which is a good alternative to the more conventional variations of the crystallization parameters normally used to this end. Decreasing the grain size through the choice of a diol with a short C chain (ethanediol) leads to the preparation of continuous films with lower thickness, i.e., the

critical thickness below which the films break up into isolated structures can be reduced to a value close to 15 nm, which corresponds to a value of the grain size to thickness ratio, $G/t < 5.0$

Acknowledgements

This work is part of the activities of the European network of excellence “Multifunctional and Integrated Piezoelectric Devices MIND” (NoE 515757) and it has been partially funded by the Spanish project MAT2007-61409. DTA/TGA was carried out at the Thermal Analysis Support Unit of the Materials Science Institute of Madrid (CSIC). Authors wish to thank Prof. J. Piqueras for the access to the facilities of the Microelectronics Laboratory of the Universidad Autónoma de Madrid and Dr. C. Ballesteros for the access to the Transmission Electron Microscopy service of the Universidad Carlos III de Madrid.

References

- [1] K.L. Ekinici: Electromechanical transducers at the nanoscale: actuation and sensing of motion in Nanoelectromechanical Systems (NEMS). *Small* **1**, 786 (2005).
- [2] J. Woo, S. Hong, D.K. Min, H. Shin and K. No: Effect of domain structure on thermal stability of nanoscale ferroelectric domains. *Appl. Phys. Lett.* **80**, 4000 (2002).
- [3] M. Park, S. Hong, J. Kim, Y. Kim, S. Bühlmann, Y.K. Kim and K. No: Piezoresponse Force Microscopy studies of PbTiO₃ thin films grown via layer-by-layer gas phase reaction. *Appl. Phys. Lett.* **94**, 092901 (2009).
- [4] J.F.Scott Applications of Modern Ferroelectrics. *Science* 315, 954 (2007).
- [5] T.M. Shaw, S. Trolier-McKinstry and P.C. McIntyre: The properties of ferroelectric films at small dimensions. *Annu. Rev. Mater. Sci.* **30**, 263 (2000).
- [6] A. Roelofs, T. Schneller, K. Szot and R. Waser: Towards the limit of ferroelectric nanosized grains. *Nanotechnology* **14**, 250 (2003).
- [7] J. Junquera and Ph. Ghosez: Critical thickness for ferroelectricity in perovskite ultrathin films. *Nature* **422**, 506 (2003).
- [8] D.D. Fong, G.B. Stephenson, S.K. Streiffer, J.A. Eastman, O. Auciello, P.H. Fuoss, and C. Thompson: Ferroelectricity in ultrathin perovskite films. *Science* **303**, 1650 (2004).
- [9] R.W. Schwartz, T. Schneller and R. Waser: Chemical solution deposition of electronic oxide films. *C.R. Chimie* **7**, 433 (2004).
- [10] A.M. Doyle, G. Rupprechter, N. Pfänder, R. Schlögl, C.E.A. Kirschhok, J.A. Martens, H.-J. Freund: Ultra-thin zeolite films prepared by spin-coating Silicalite-1 precursor solutions. *Chem. Phys. Lett.* **382**, 404 (2003).

- [11] A. Hardy, S. Van Elshocht, J. D'Haen, O. Douthéret, S. De Gendt, C. Adelmann, M. Caymax, T. Conard, T. Witters, H. Bender, O. Richard, M. Heyns, M. D'Olieslaeger, M.K. Van Bael and J. Mullens: Aqueous chemical solution deposition of ultrathin lanthanide oxide dielectric films. *J. Mater. Res.* **22**, 3484 (2007).
- [12] T. Kijima and H. Ishiwara: Si-substituted ultrathin ferroelectric films. *Jpn. J. Appl. Phys. Part 2* **41**, L716 (2002).
- [13] A. González, R. Jiménez, J. Mendiola, C. Alemany and M.L. Calzada: Ultrathin ferroelectric strontium bismuth tantalate films. *Appl. Phys. Lett.* **81**, 2599 (2002).
- [14] J. Celinska, V. Joshi, S. Narayan, L. McMillan and C.A. Paz de Araujo: Effects of scaling the film thickness on the ferroelectric properties of $\text{SrBi}_2\text{Ta}_2\text{O}_9$ ultra thin films. *Appl. Phys. Lett.* **82**, 3937 (2003).
- [15] G.L. Brennecka and B.A. Tuttle: Fabrication of ultrathin film capacitors by chemical solution deposition. *J. Mater. Res.* **22**, 2868 (2007).
- [16] J. Ricote, S. Holgado, P. Ramos and M.L. Calzada: Piezoelectric ultrathin lead titanate films prepared by deposition of aquo-diol solutions. *IEEE Trans. Ultrason. Ferroel. Freq. Control* **53**, 2299 (2006).
- [17] J. Ricote, S. Holgado, Z. Huang, P. Ramos, R. Fernández and M.L. Calzada: Fabrication of continuous ultrathin films ferroelectric films by Chemical Solution Deposition Methods. *J. Mater. Res.* **23**, 2787 (2008).
- [18] J. Sigman, G.L. Brennecka, P.G. Clem and B.A. Tuttle: Fabrication of perovskite-based high-value integrated capacitors by chemical solution deposition. *J. Am. Ceram. Soc.* **91**, 1851 (2008).
- [19] K.T. Millar, F.F. Lange and D.B. Marshall: The instability of polycrystalline thin films: Experiment and theory. *J. Mater. Res.* **5**, 151 (1990).

- [20] A. Seifert, A. Vojta, J.S. Speck and F.F. Lange: Microstructural instability in single-crystal thin films. *J. Mater. Res.* **11**, 1470 (1996)
- [21] L. Zhao, A.T. Chien, F.F. Lange and J.S. Speck: Microstructural development of BaTiO₃ powders synthesized by aqueous methods. *J. Mater. Res.* **11**, 1325 (1996)
- [22] W.T. Lee, E.K.H. Salje and M.T. Dove: Effect of surface relaxations on the equilibrium growth morphology of crystals: platelet formation. *J. Phys.: Condens. Matter* **11**, 7385 (1999)
- [23] P.A. Langjahr, T. Wagner, M. Rühle and F.F. Lange: Thermally induced structural changes in epitaxial SrZrO₃ films on SrTiO₃. *J. Mater. Res.* **14**, 2945 (1999)
- [24] M. Dawber, I. Szafraniak, M. Alexe and J.F. Scott, Self-patterning of arrays of ferroelectric capacitors: description by theory of substrate mediated strain interactions. *J. Phys.: Condens. Matter* **15**, L667-L671 (2003)
- [25] N.J. Phillips, M.L. Calzada and S.J. Milne: Sol-gel-derived lead titanate films. *J. Non-Cryst. Solids* **147-148**, 285 (1992).
- [26] Z. Huang: Combining Ar ion milling with FIB lift-out techniques to prepare high quality site-specific TEM samples. *J. Microsc.* **215**, 219 (2004).
- [27] Y.L. Tu, M.L. Calzada, N.J. Phillips and S.J. Milne: Synthesis and electrical characterization of thin films of PT and PZT made from a diol-based sol-gel route. *J. Am. Ceram. Soc.* **79**, 441 (1996).
- [28] M.L. Calzada and R. Sirera: Chemically derived ferroelectric calcium modified lead titanate thin films deposited from aquo-diol-solvent solutions. *J. Mater. Sci.* **7**, 39 (1996).

List of tables

| Láminas PT | 0.30M | 0.20M | 0.15M | 0.10M | 0.05M |
|--------------------------|--------------|--------------|--------------|--------------|--------------|
| diol dilution | 2.8 | 3.9 | 4.0 | 4.4 | 8.9* |
| water dilution | 2.7 | 2.9 | -- | 4.4 | 6.2* |
| ethylhexanol dilution | | | | | |
| <i>etanediol route</i> | -- | 3.7 | 4.6 | 4.7 | 8.6* |
| <i>propanediol route</i> | -- | 4.2 | 4.7 | 6.2* | 10.4* |
| <i>pentanediol route</i> | -- | 4.4 | 6.0* | 8.9* | 16.0* |

Table 1. G/t values of PbTiO₃ films obtained from solutions with different concentrations and using different solvents for dilution and different types of diols in their preparation. (* Discontinuous film).

Figure captions

Figure 1. Evolution of film thickness with the concentration of the precursor solution for PbTiO_3 -based films. Previous results of films obtained from solutions diluted in water or diol [16,17] are compared with those for which ethylhexanol is used. The figure also shows the observed critical thickness below which the coating of the substrate is incomplete.

Figure 2. DTA and TGA curves corresponding to gels obtained for PbTiO_3 solutions 0.3M diluted in a) diol; b) water and c) ethylhexanol.

Figure 3. Grazing incidence X ray diffraction diagrams of PbTiO_3 ultrathin films obtained from the deposition of diluted solutions with different concentrations using: a) 1,2 etanediol; b) 1,3 propanediol and c) 1,5 pentanediol.

Figure 4. Evolution of the film thickness (determined by ellipsometry) with the concentration of the precursor solution for three series of films synthesised using different types of diols.

Figure 5. SFM topography images of the surfaces of PbTiO_3 films obtained from solutions synthesized using 1,2 etanediol and with different concentrations: a) 0.20 M; b) 0.15 M; c) 0.10 M; d) 0.05 M.

Figure 6. SFM topography images of the surfaces of PbTiO_3 films obtained from solutions synthesized using 1,3 propanediol and with different concentrations: a) 0.20 M; b) 0.15 M; c) 0.10 M; d) 0.05 M.

Figure 7. SFM topography images of the surfaces of PbTiO_3 films obtained from solutions synthesized using 1,5 pentanediol and with different concentrations: a) 0.20 M; b) 0.15 M; c) 0.10 M; d) 0.05 M.

Figure 8. Transmission electron microscopy images of cross sections of PbTiO_3 films obtained from solutions based on etanediol: a) 0.20 M; b) 0.10 M; c) 0.05 M

Figure 9. Transmission electron microscopy images of cross section of PbTiO_3 films obtained from solutions based on propanediol: a) 0.20 M; b) 0.10 M; c) 0.05 M

Figure 10: Transmission electron microscopy images of cross section of PbTiO_3 films obtained from solutions based on pentanediol: a) 0.20 M; b) 0.15 M; c) 0.10 M

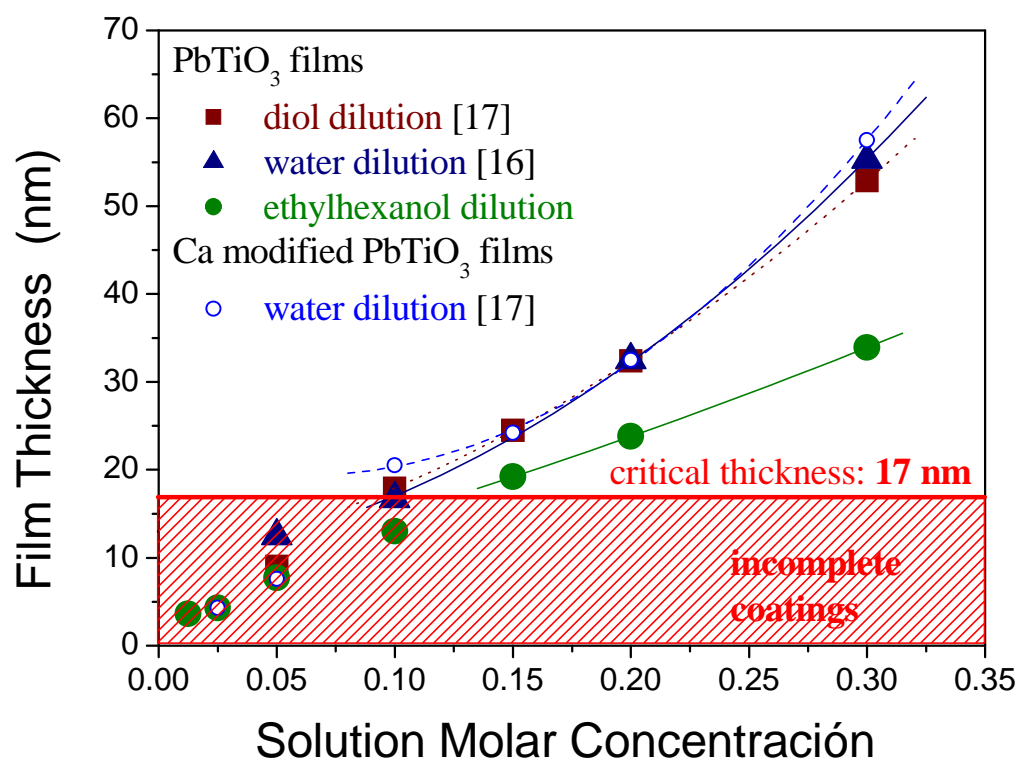


Figure 1

R. Fernández et al.

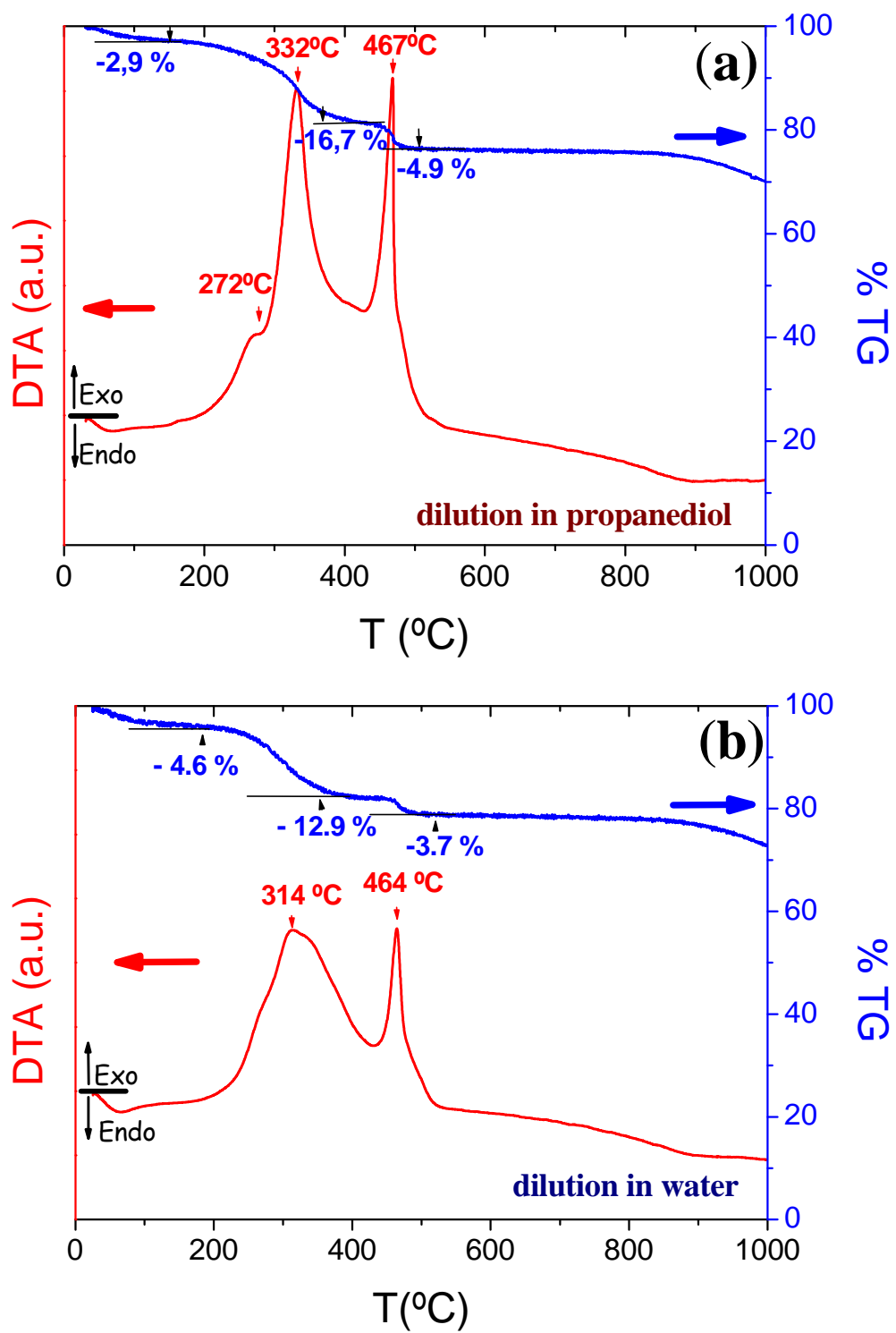


Figure 2
R. Fernández et al.

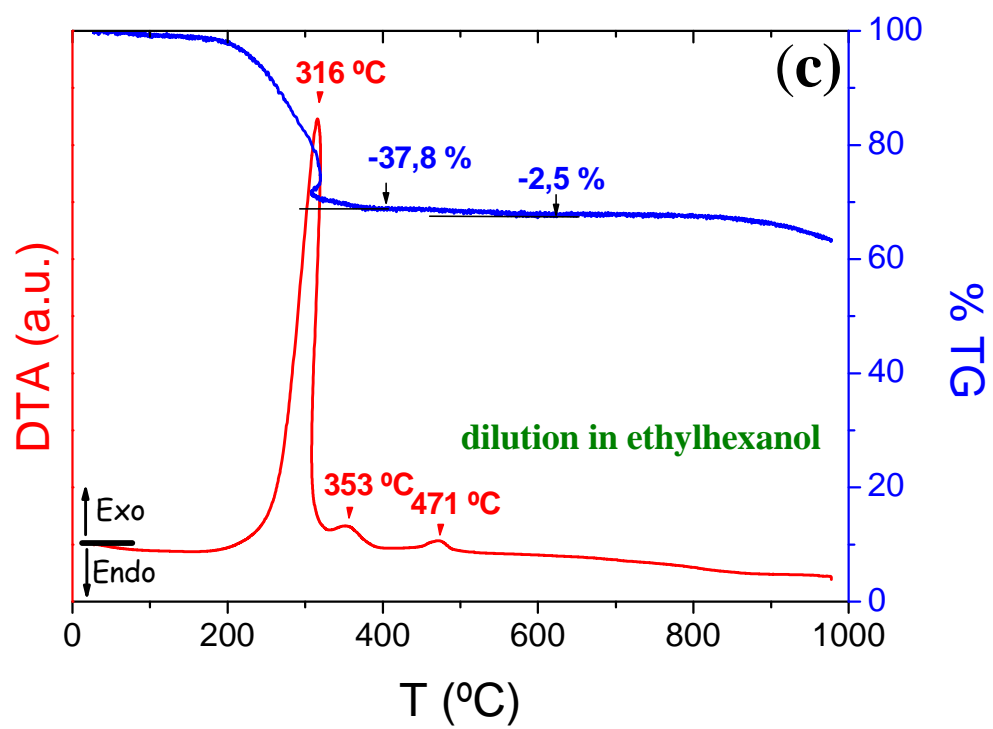


Figure 2
R. Fernández et al.

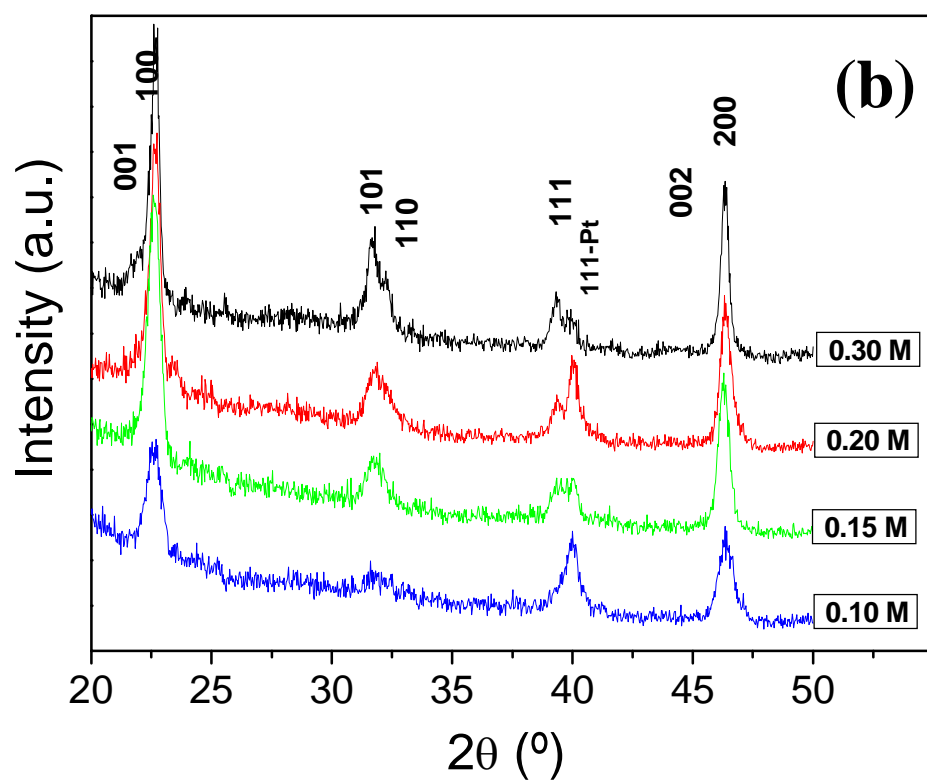
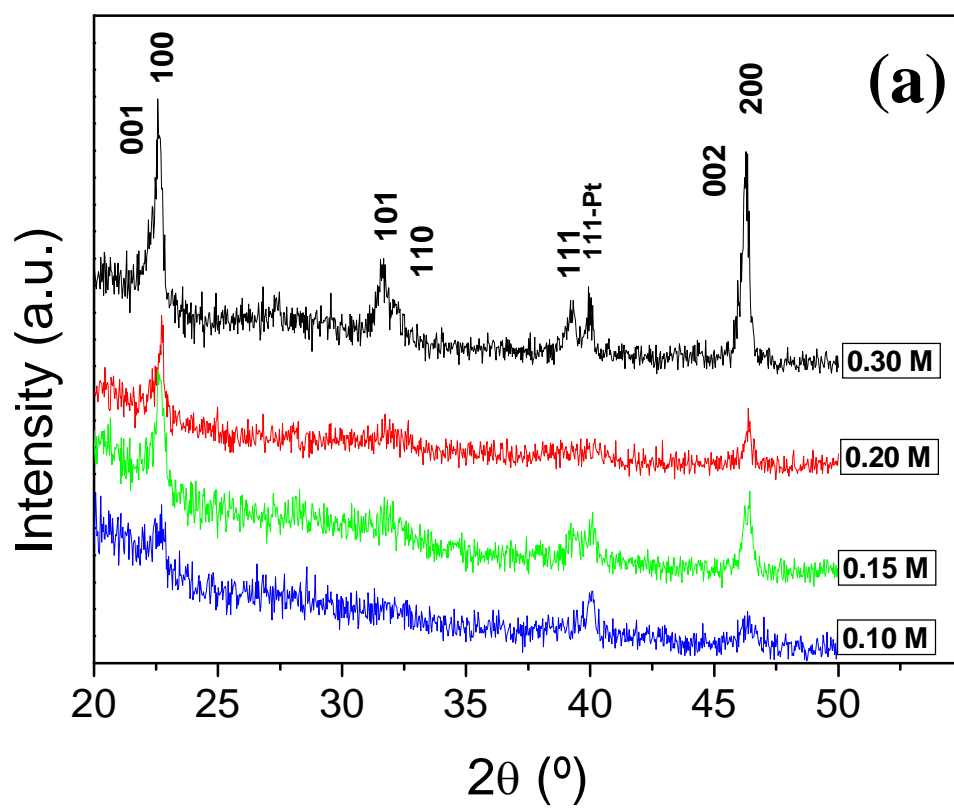


Figure 3

R. Fernández et al.

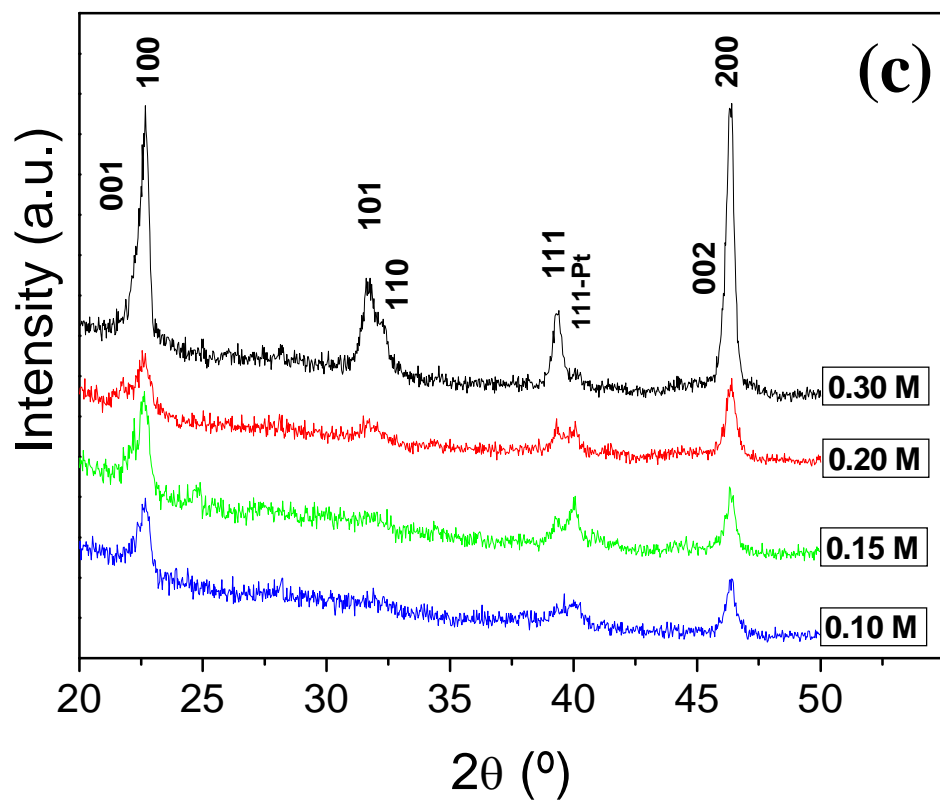


Figure 3
R. Fernández et al.

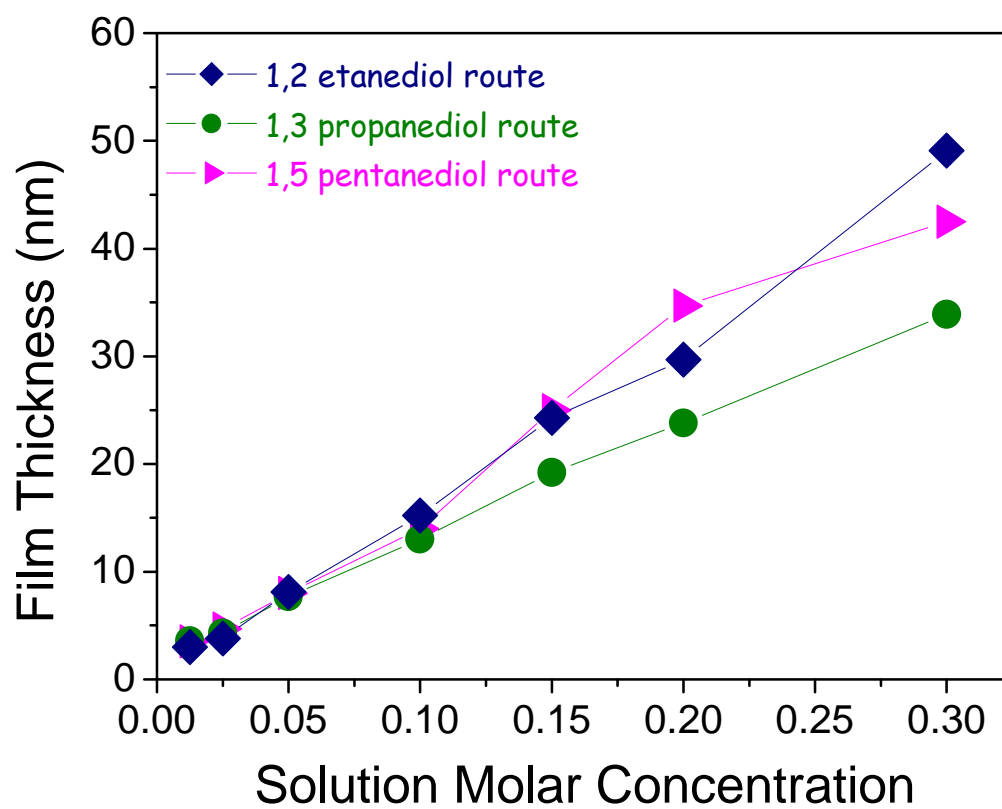


Figure 4

R. Fernández et al.

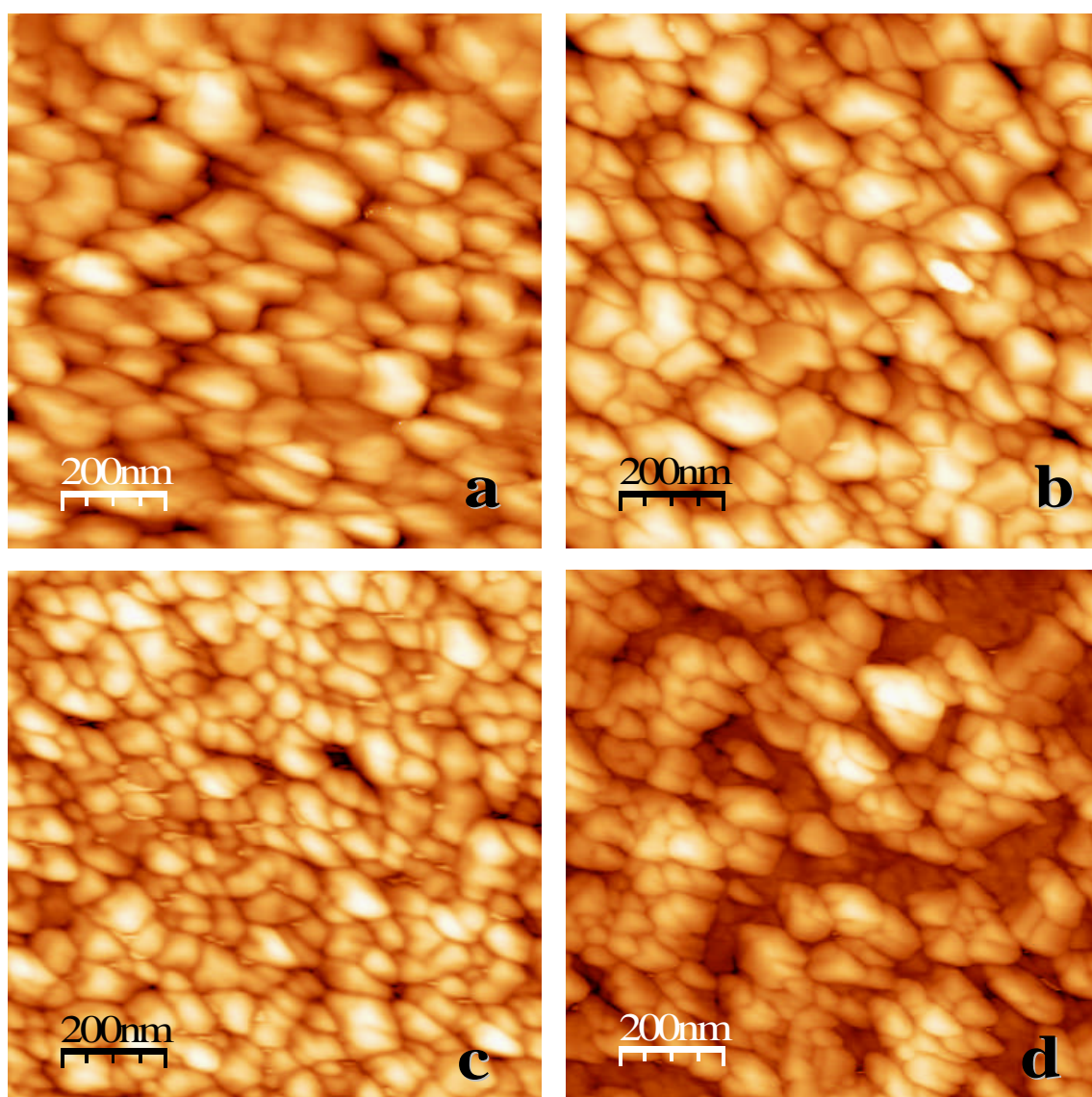


Figure 5
R. Fernández et al.

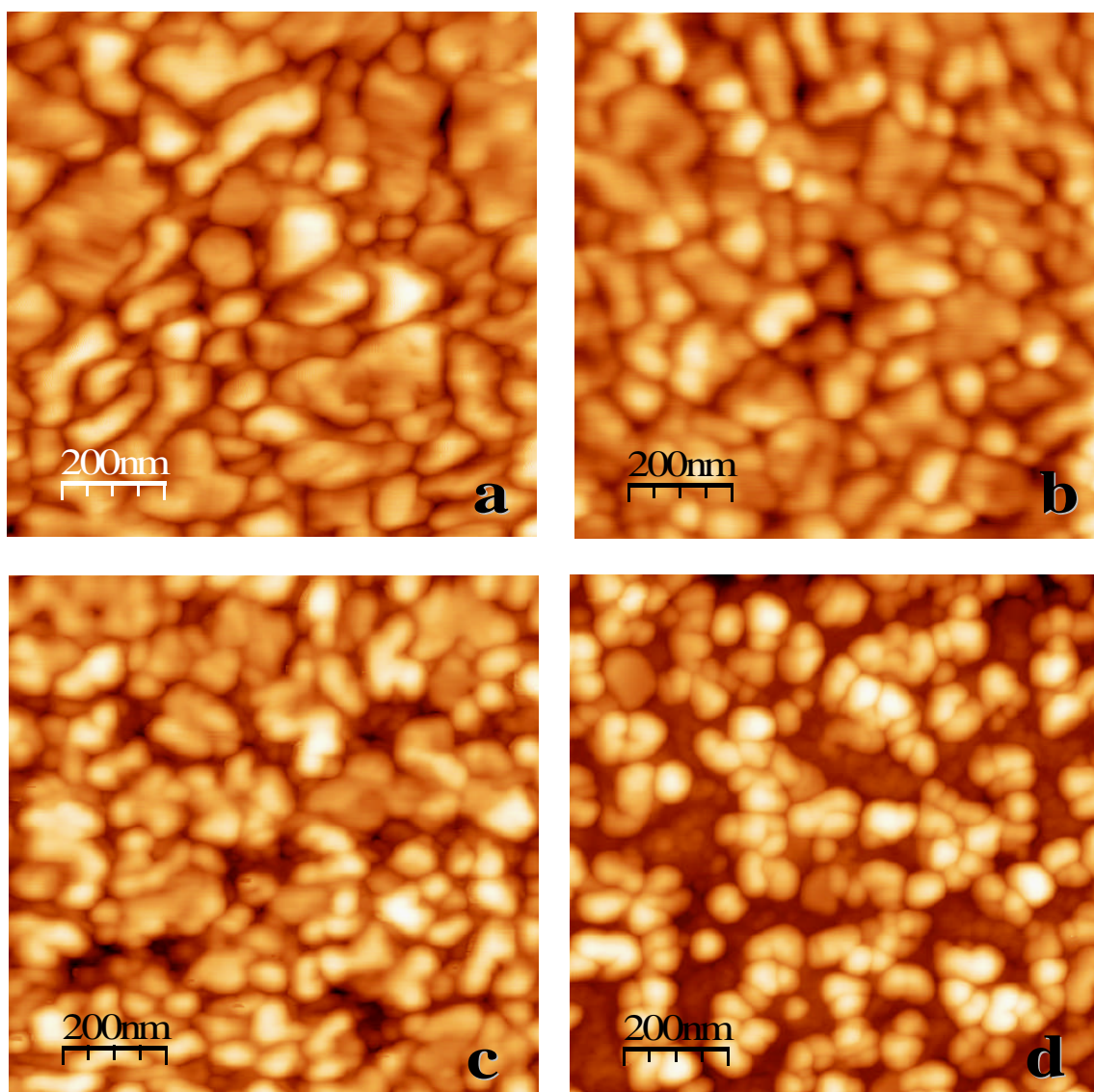


Figure 6
R. Fernández et al.

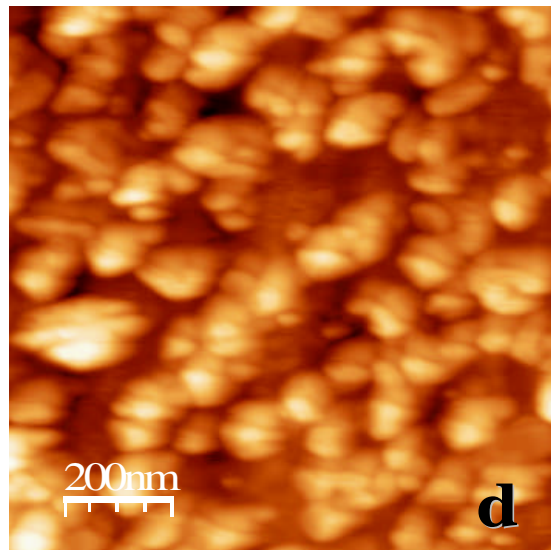
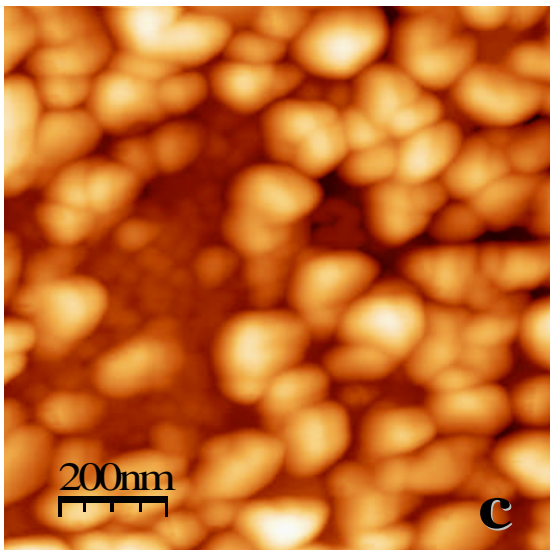
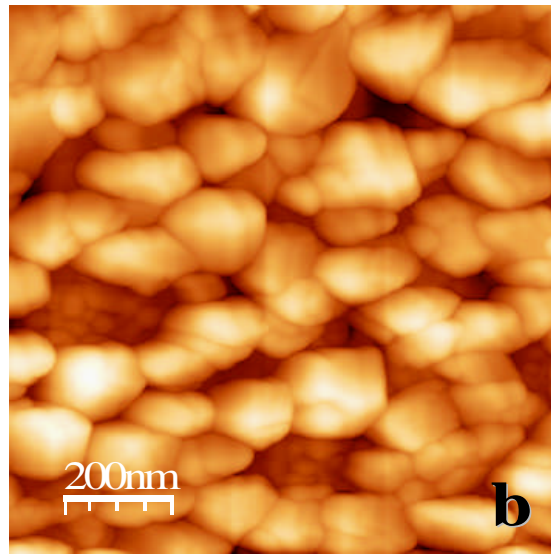
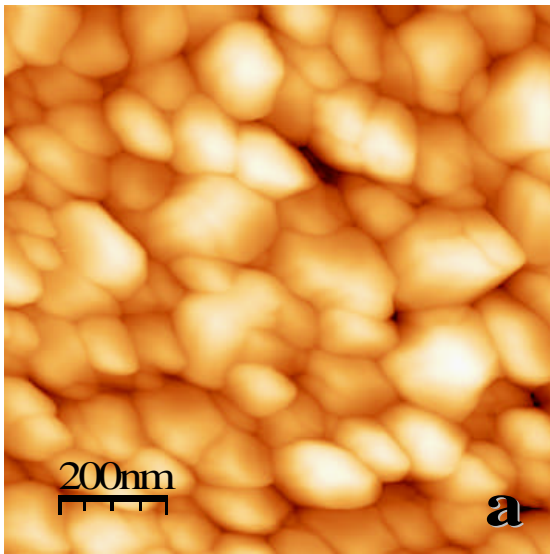


Figure 7
R. Fernández et al.

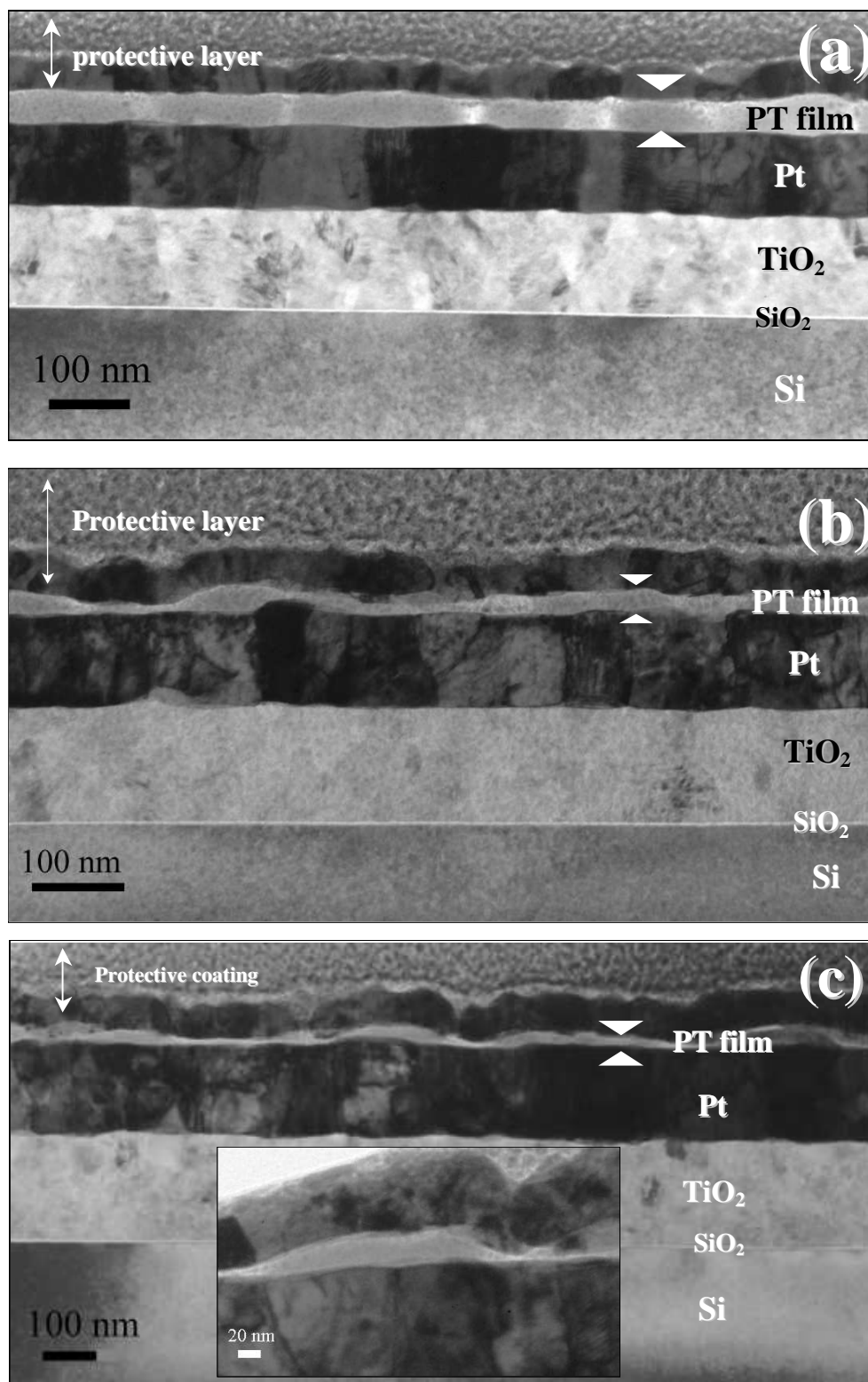


Figure 8

R. Fernández et al.

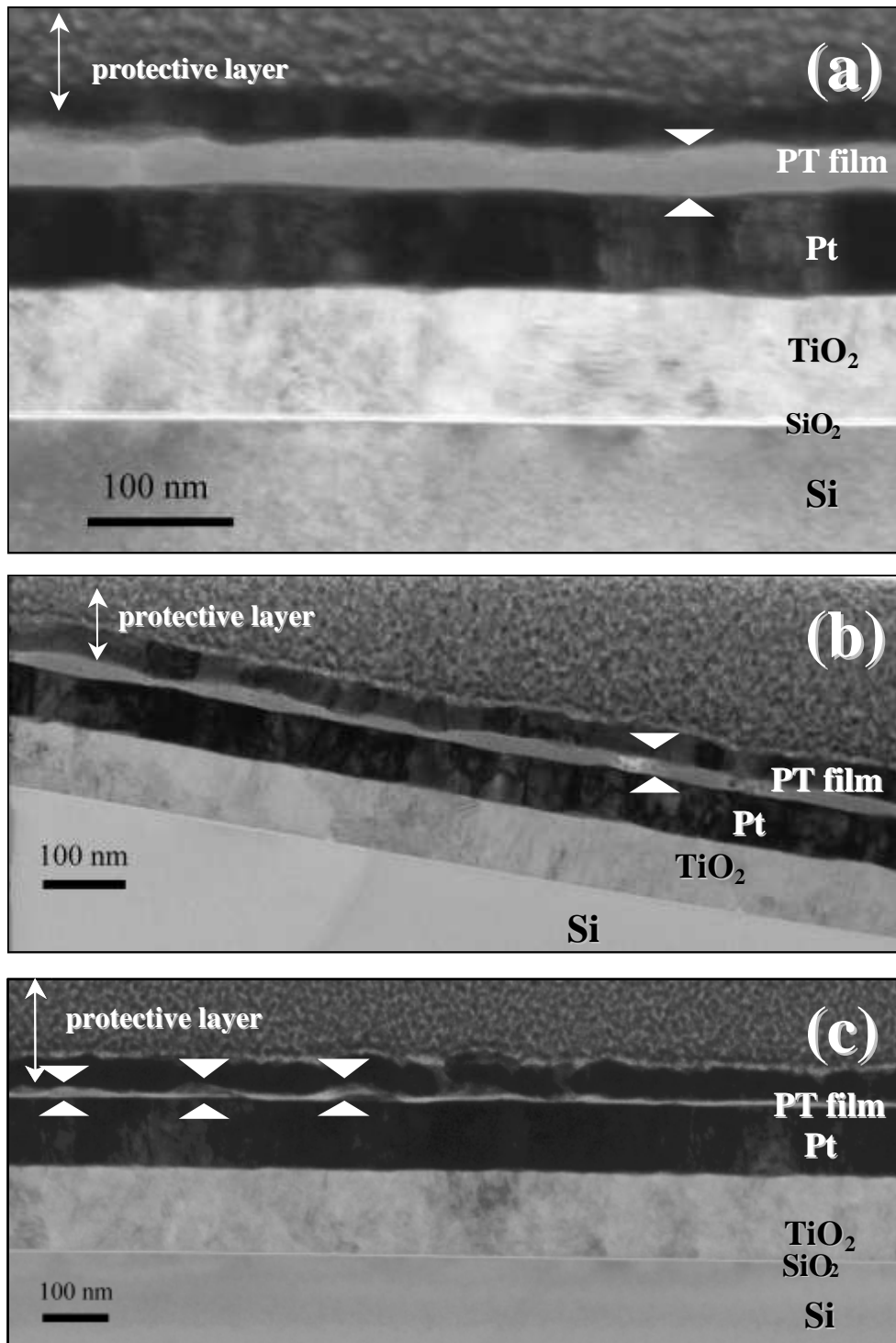


Figure 9
R. Fernández et al.

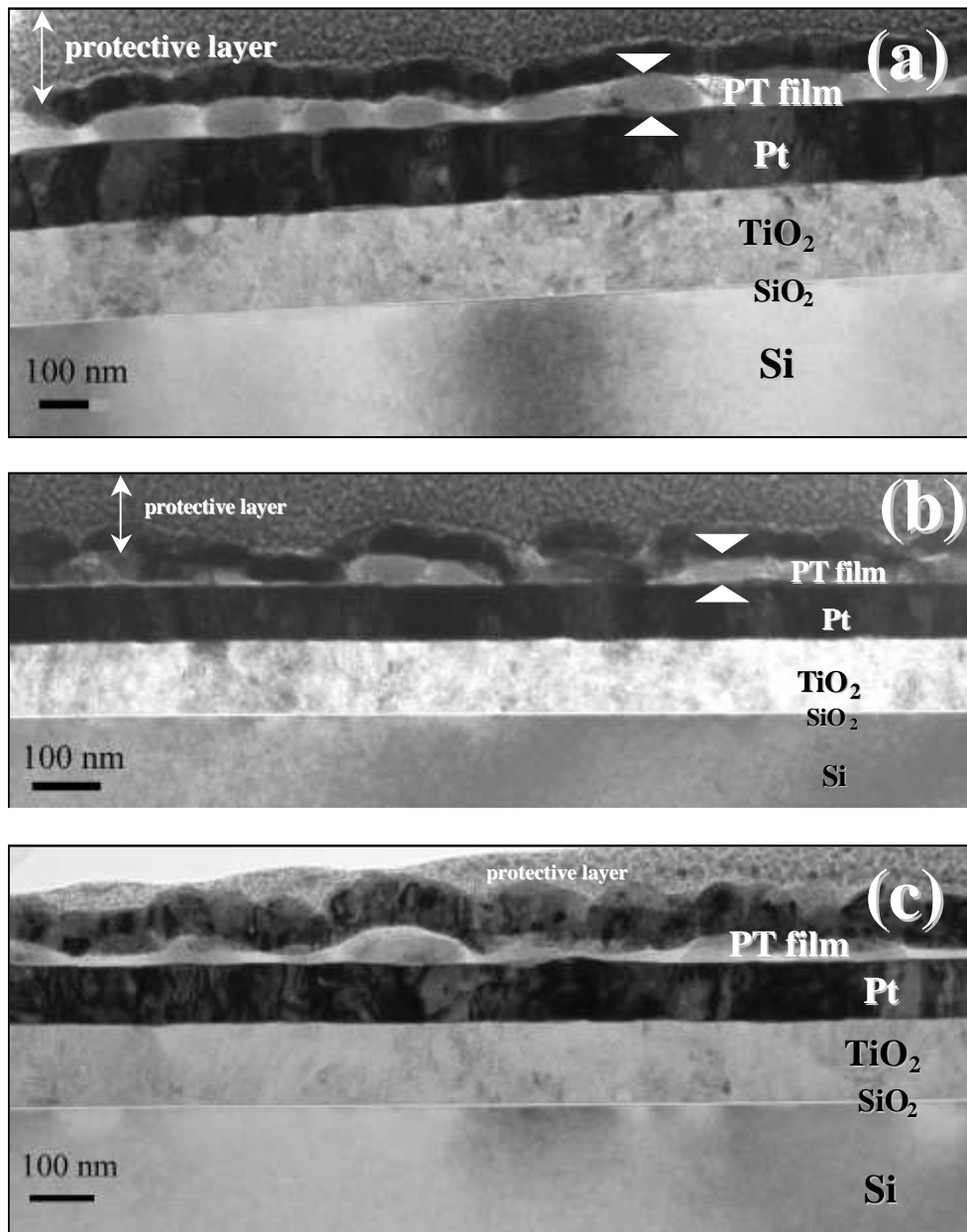


Figure 10
R. Fernández et al.